ENGINEERING RESEARCH JOURNAL (ERJ)

Vol. 1, No. 48 Apr. 2021, pp. 59-73

Journal Homepage: http://erj.bu.edu.eg

Zinc-Magnesium Based biodegradable Alloys for bone plate application

Khaled Waly[a], Mohamed Tarek Elwakad[b], Madyha Shoieb[c], Mohamed Mousa[c], Amal S. Eldesoky[a]

a Department of Biomedical Engineering, Higher Technological Institute, 10th of Ramadan, 228, Egypt.

b Faculty of Engineering & Technology, Future University , Fifth settlement, Cairo, Egypt

cCentral Metallurgical Research and Development Institute (CMRDI), P.O. Box 87, Helwan, Cairo, Egypt

Corresponding author: amal-eldesoky70@hotmail.com, Tel: +2 01097884690

Abstract

In this paper, Zinc-based alloys with different ratios of Mg (magnesium) were fabricated as degradable bone plate for medical applications. Zinc with Mg percentages (0.5, 1.0, 1.5 and 2.0 wt. %) were prepared. Compatibility assurance study was done to measure the suitability to be used as degradable bone plates. Composition and microstructure of Zn-Mg alloy were investigated by SEM (scanning electron microscope) and EDS (energy dispersive spectrometer). Density, hardness, and compression strength were measured. The corrosion resistance in SBF (simulated body fluid) were measured, also. Good microstructure, the highest hardness and wear resistance were observed for alloy with 0.5% Mg. Measurements indicated that the density decreases with increasing Mg by 10.4% and 14%. Corrosion resistance was improved 71.68 % for 0.5 % Mg compared to pure Zn. Hardness and compression enhanced by addition of Mg, while the highest wear resistance achieved for 0.5 wt. % Mg. Tensile strength of Zn–Mg alloy were enhanced from 39 MPa for pure zinc to 320 MPa and 300 MPa for Zn–0.5 Mg alloy and Zn–2Mg alloy. This can be explained due to preparation process and presence of Mg + MgZn mixture in the structure. Compression strength of Zn–Mg alloy were enhanced from 65-75 MPa for pure zinc to 600 MPa and 620 for Zn–0.5 Mg alloy and Zn–2Mg alloy. No change in weight was detected for the different plates after immersion test.

Zinc alloy with 0.5 % Mg magnesium has the highest mechanical biocompatibility that approaches mechanical properties of cortical bone and exceeded. It has the highest corrosion resistance. So, it is a suitable degradable material could be used for dental and bone plates applications.

Keywords: Biocompatibility; zinc alloy; degradation implant; Corrosion; magnesium.

1. Introduction

Nowadays, biomaterials have a main role in various biomedical applications engineering. There are requirements for that material used in contact with patient should be satisfied [1-2]. In-Vivo applications may require biodegradable materials to avoid other surgery for removing it [3]. Magnesium (Mg) considered a pioneer biomaterial used as a degradable. Magnesium plate's density ranged from 1.8 to 2 g/cm3 and has mechanical properties similar to properties of bone. Magnesium as degradable bone plate lose its mechanical strength with rate greater than rate of cell growth [4-6]. For its high degradation rate by means of low corrosion resistant, processing is need to control the corrosion rate that also effects on mechanical

properties as hardness, tensile strength, and compression strength [6-7]. Magnesium and Zinc are natural metals found in body. Now, Zinc is an attractive degradable material used for tissue engineering and biomedical applications. Unlike Magnesium, Zinc has low melting point that enables easy fabrication. It also has low tensile strength and low costs [8]. Zinc alloy plates have superior low corrosion resistant and mechanical properties for some applications [8-13]. Product of corrosion should be controlled to avoid toxicity as a result of high zinc concentration [14- 16].

Few years ago, zinc alloys had great attention. Using Zinc as pure material is limited as it has poor tensile strength and hardness. Zinc alloy shows some toxicity for different cell type [17-19]. For example, Zn-3Mg alloy shows decreasing viability of cells with limited biocompatibility [20–25]. Alloy composed of Mg–Zn–Ca shows some compatibility, and decreased hydrogen evolution. Presence of MgZn eutectic with Mg decreases mechanical properties [26-28]. Corrosion rate decreased for zinc based alloy compared to pure zinc [23, 29-30]. Recently, investigations are done for using zinc based-XMg alloy for degradable orthopedics application [31-33].

This investigation deals with mechanical and corrosion for biocompatibility studies of Zinc based alloy reinforced with magnesium with various weight percentages for orthopedic applications.

2. Experimental Methods and Procedures

2.1 Material Preparation

Zinc based Magnesium alloy were prepared with various Mg ratios of 0.5, 1, 1.5 and 2 wt. % using pure Zn (99.995 wt.%) and pure magnesium(99.8 wt.%). Melting was performed at 500°C in a graphite crucible placed in an electric resistance furnace. A protective Argon gas was employed during melting and casting processes to avoid oxidation and contamination,. Stirring for 3 min using stainless steel rod to achieve homogenization, then hold for 15 min for complete metals homogenization. It is meaningless, the slag was removed and the melt was poured at 500°C into a preheated cast iron mold. The mold was hollow cylinder with outer diameter of 100 mm, inner diameter of 50 mm and 250mm length. The chemical analysis was performed using X-ray fluorescence (XRF) analyzer,(Axios advanced-PANALYTICAL, Netherlands). The chemical compositions of the alloys are shown in Table-1.

Table 1: Chemical composition of the prepared alloys in wt. %

Alloy code	Zn	Mg	Fe	Cu
Zn	Bal.	-	0.015	0.002
Zn-0.5Mg	Bal.	0.47	0.021	0.0015
Zn-1Mg	Bal.	1.15	0.023	0.0021
Zn-1.5Mg	Bal.	1.45	0.021	0.0018
Zn-2Mg	Bal.	1.96	0.022	0.0016

2.2 Materials Characterization

2.2.1. Microstructure

Disks with thickness 10 mm were cut for microstructure investigations. Then grinding was performed on sandpapers up to 1200 grit. The specimens were polished using alumina suspension of particle size 2µm and distilled water. Nital solution composed of 95 % ethanol and 5 % nitric acid was used for specimens to reveal the microstructure. Immersion specimens in solution for 40 sec. then dried in blast of dried air. Optical microscope (OM) (model OPTIKA M-790, Italy) was used for metallographic observations. Five OM micrographs were taken for each specimen at low magnification of 200x. The average size of the Zn-

Mg grains was measured by image analyzer AxioVision SE64 Rel. 4.9 software.

2.2.2. Physical Properties Measurements

The density of the compositions were calculated using theoretical density values for zinc (7.13g/cm3), and Mg (1.8-2.0 g/cm3) using equation below [34].

$$\rho_{th.} = \frac{100}{\left(\frac{w_m}{\rho_m}\right)+\left(\frac{w_1}{\rho_1}\right)} \quad (1)$$

Where, ρth, ρm, and ρ1are the theoretical density, matrix, and the dispersed phase, respectively. Wm and W1 are the weight percent of the matrix and the dispersed phase. On other hand, the sintered materials densities were determined using Archimedes principal according to ASTM C 373-72, 1984 according to equation -2 [34].

$$\rho_{Arch.} = \frac{w_{air}}{(w_{air}-w_{water})} \quad (2)$$

Where, Wair and Wwater are the samples weight in air and water, respectively.

To study microstructure, morphology and element distribution, the sample was polished using SiC papers. Then, the surface was polished with three micro-meter particle size diamond paste. QUANTA FEG250-EDAX Genesis SEM equipped with an energy X-ray micro-analyzer (EDS) was used. Samples composition were investigated using Brukur X-ray diffractometer [D8 kristalloflex (Ni-filtered Cu Ka)].

2.2.3 Mechanical properties investigation

Hardness of prepared samples were measured using Vickers hardness tester (Matsuzawa JAPAN) by applying 20 kg load for 15 sec loading time at room temperature. The test was repeated five times for each alloy and result values were averaged.

The test conditions are given in Table-2. The samples and the ring of machine were cleaned using ultrasonic and acetone for washing. Wear rate was studied by recording the weight and the loss with sensitivity of 0.0001 gm. The value was recorded twice and averaged.

Table 2: **test conditions**

Test condition	Apply 20 kg load for 15 sec at room temperature
Specimen radius	10 mm
Specimen high	12 mm
Disc material	Stainless steel-62 HR

Tensile strength and compression strength were measured using universal testing machine with rate of 1mm/min according to standard test method.

2.2.4 Electrochemical Measurements

Corrosion rate and electrochemical measurements of Zn-Mg implants are measured at room temperature using electrochemical working station (AUTOLAB, PGSTA30, Netherlands). The used electrolyte was simulated body fluid (SBF) with shown composition in Table 3 [35]. Each sample of the surface area 0.785 cm^2 is polished before the test. In the test, a platinum counter electrode and a saturated calomel reference electrode (SCE) were used.

The open-circuit potential (OCP) of each sample was monitored for 0.5 hr in SBF. Then, the potentiodynamic polarization test is measured with a scan rate of $2mVs^{-1}$. Corrosion parameters including corrosion potential (E_{corr}) and corrosion current density (I_{corr}) are estimated from the polarization curves by Tafel analysis based on the polarization plots.

Table 3: Composition of simulated body fluid (SBF)

Material	Amount
NaCl	8.0g
NaHCO3	0.35g
KCl	0.25g
K2HPO4.3H2O	0.25g
MgCl2.6H2O	0.30g
1M.HCl	50ml
CaCl2	0.30g
NaSO4	0.08g
(CH2OH)3CNH2	6.00g

The immersion test is carried out according to ASTM-G31-72 [36], where each Zn-Mg sample immersed in 100 ml solution for 21 days at room temperature.

3. Result and Discussion

3.1. Physical characterization

3.1.1 Microstructure characterization

Fig. 1 presents the OM microstructures of pure Zn and Zn-XMg alloys with different Mg content. The pure Zn in Fig. 1a contains large Zn dendrites with an average dendrite length of about 550 µm. With Zn-XMg alloys, the microstructures consist of the primary Zn dendrites (light) and eutectic mixture of Zn andMg2Zn11 (dark) as shown in Figs. 1b-e. Fig. 2 shows the variation of with average dendrite length of the primary Zn dendrites with Mg content [37]. With addition of 2 wt% Mg, the fine primary Zn dendrites are formed and their average length reduced to about85µm as shown in Fig. 2.

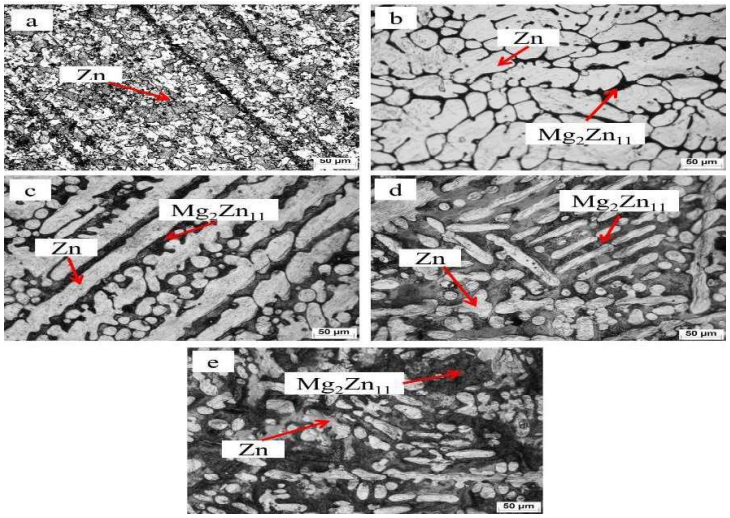

Fig. 1:The OM microstructures of (a) pure Zn and Zn-XMg alloys with different Mg content: (b) 0.5 wt%, (c) 1wt%, (d) 1.5 wt% and (e) 2 wt%.

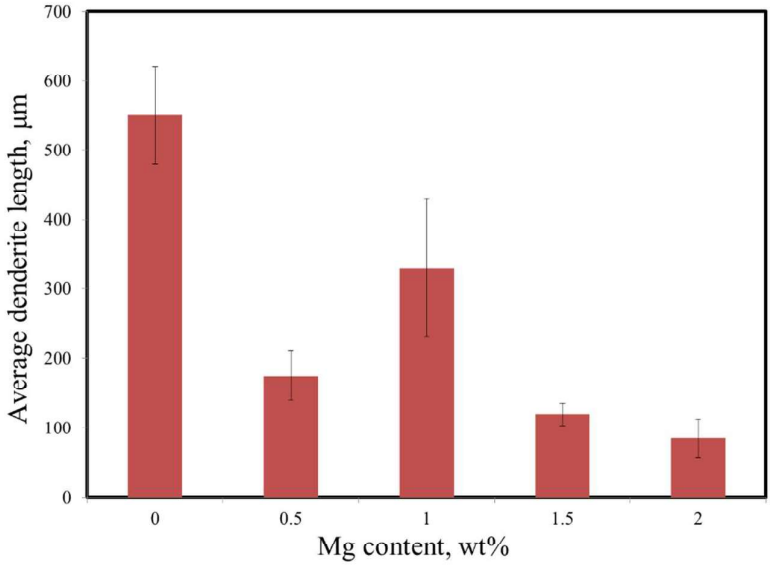

Fig. 2: average dendrite length of the primary Zn dendrites with Mg content.

3.1.2. Density measurements

The experimental densities Zn-Mg are shown in Figure 3. It shows that the theoretical densities of pure zinc sample decreased gradually by increasing Mg content. When the density of Mg is lower than the density of zinc, the total density of the composite decreased. The density of Mg (1.9 g/cm3) is lower than density of Zn (7,13 g/cm3) matrix. So, the overall density of alloy decreased according to percentage of Mg. Density decreased by range of 4% to 8.83% according to Mg percentage. As, no porosity sample is difficult to obtain, the effect of this point should be considered. Compaction pressure, melting temperature and sintering time are factors effect on density. Figure-3 shows the measured densities. Also, agglomerations of Mg causing presence some pores may decrease the density value.

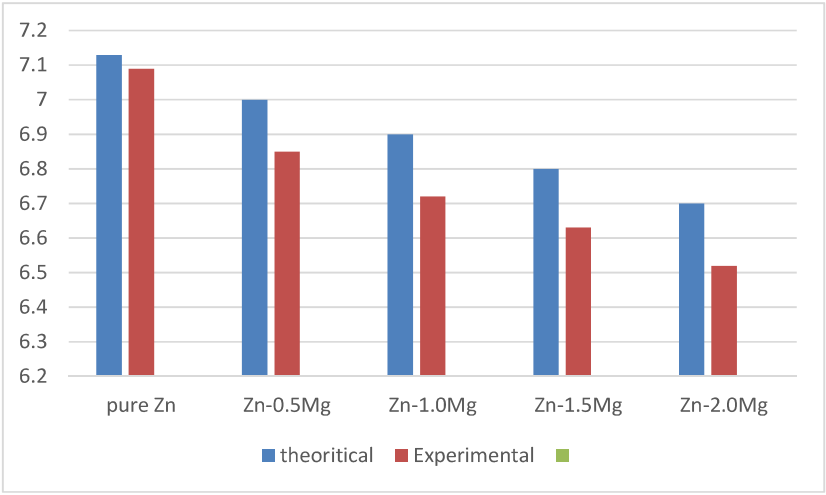

Fig. 3: The densities of Zn sample with different Mg ratios

3.1.3. Composites microstructure

The SEM images of the Zn-Mg samples are shown in Figure.4. Excellent adhesion is clear at the interface between the two materials (Zn and Mg). Lamellar structures are seen in some images. Lamellar structures were not affected by changing Mg content as shown in Fgure.4. It is clear from image. Excellent distribution of constituents is achieved in all samples. Some agglomerations formed by increasing the Mg percent that may cause pores. Mg was completely diffused in the zinc and some agglomerations are observed in the sample with 2.0 wt. % Mg.

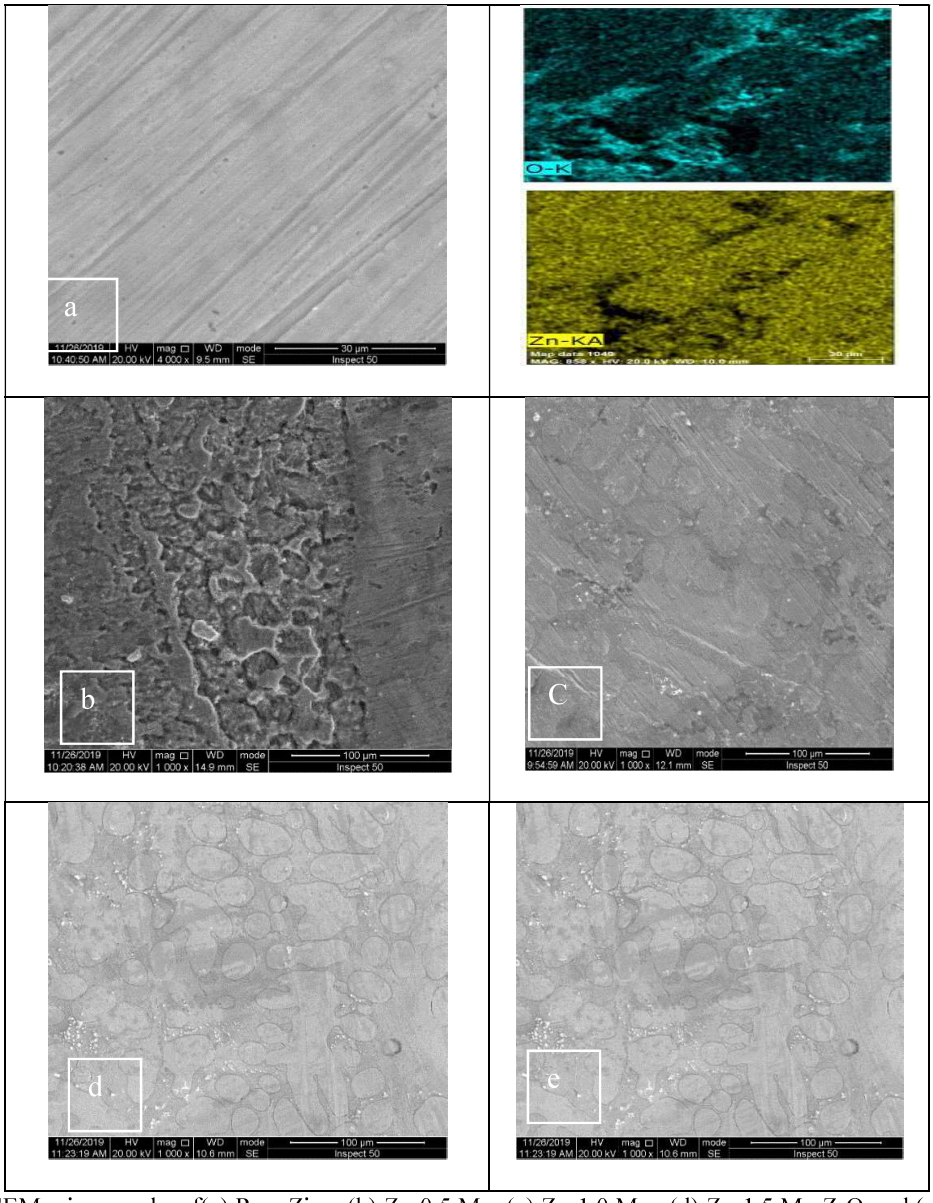

Fig.4 SEM micrographs of(a) Pure Zinc, (b) Zn-0.5 Mg, (c) Zn-1.0 Mg., (d) Zn-1.5 Mg $ZrO_2$and (e) Zn-2.0 Mg samples

Mapping was performed for all samples and the images show distribution of the constituents over samples. The distribution of Zn, Mg, and O are shown in Figure.5. Excellent distribution of all components were observed. Porosity was shown as black spots with few agglomerations.

ENGINEERING RESEARCH JOURNAL (ERJ)

Vol. 1, No. 48 Apr. 2021, pp. 59-73

Journal Homepage: http://erj.bu.edu.eg

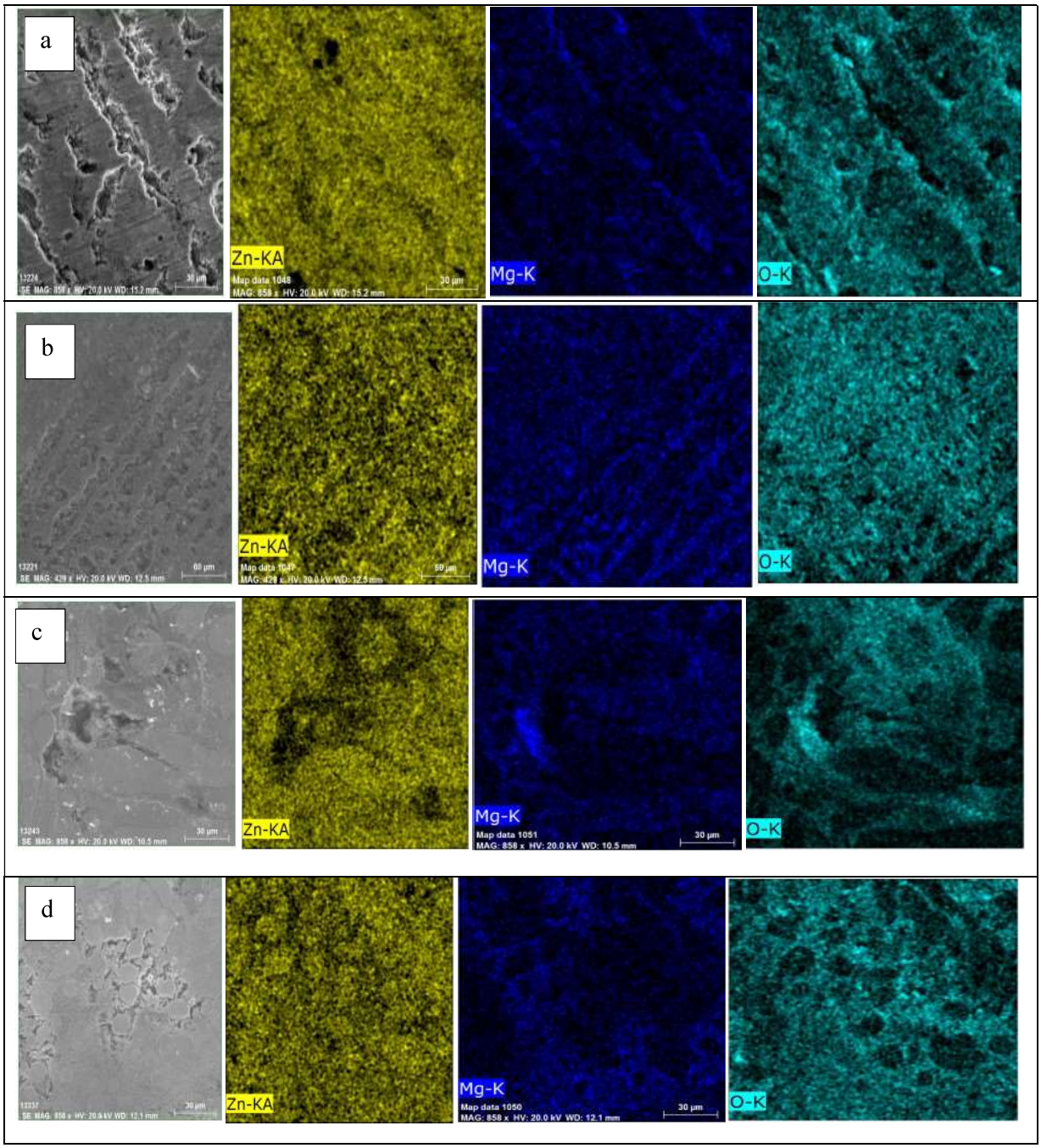

Fig. 5: SEM mapping of (a) Zn-0.5 Mg,(b) Zn-1.0 Mg,(c) Zn-1.5 Mg ZrO_2 and (d) Zn-2.0 Mg samples

EDAX analysis on all samples were done at different regions as shown in Figure 6. Regions involved peaks of zinc, magnesium, and oxygen. Images show good distribution and homogeneity in samples. No impurities were detected.

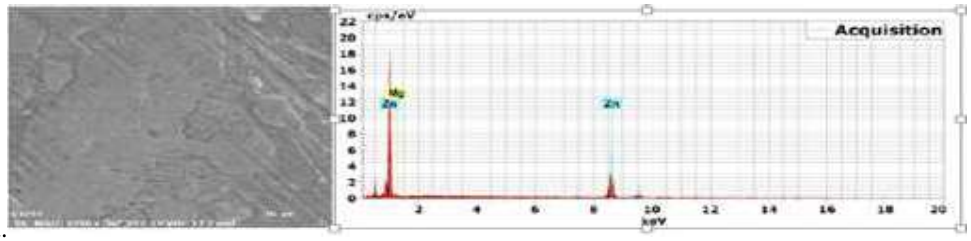

Fig. 6 SEM/EDAX analysis of Zn-0.5%Mg samples.

3.1.4. Hardness test

The effect of magnesium on hardness of pure zinc is shown in Figure.7. As shown from the figure, addition of 0.5 wt. % Mg increases hardness from 39(±2.2) to 78 (±1.7) [38]. Hardness gradually increased with increasing the percentage of Mg. Due to magnesium agglomerations that causes the presence of porosity, measuring value decreased in some samples but still within the desired range for bone implants [39].

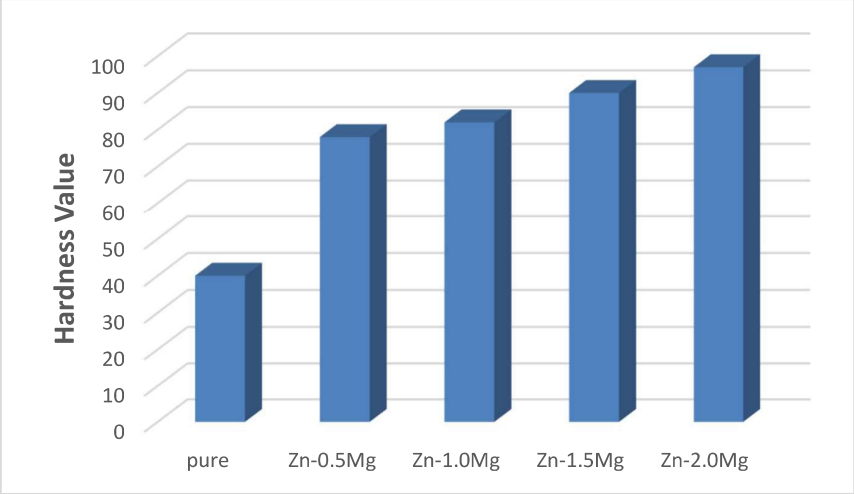

Fig.7: Hardness of the Zn alloy.

3.1.5. Mechanical properties

The wear rate of Zinc alloy was done with 20N, 300 r.p.m. for 30min. Wear rate decreased with the addition of 0.5 Mg compared to pure zinc due to the high hardness achieved with adding magnesium. Also, this may be related to the homogeneous distribution of magnesium. Other magnesium ratios show higher wear rate may be attributed porosity and agglomeration.

Tensile strength of Zn–Mg alloy were enhanced from 39 MPa for pure zinc to 320 MPa and 300 MPa for Zn–0.5 Mg alloy and Zn–2Mg alloy as shown in Figure.8. These values were higher compared to 270 MPa for Zn–1Mg. This may be explained due to process and presence of Mg + MgZn mixture in the structure that is brittle. Figure.9 shows that Compression strength of Zn–Mg alloy were enhanced from 65-75 MPa for pure zinc to 600 MPa and 620 for Zn–0.5 Mg alloy and Zn–2Mg alloy. For other magnesium ratio, compression strength was 570 and 550. These values of strength are still close to that required for bone implants.

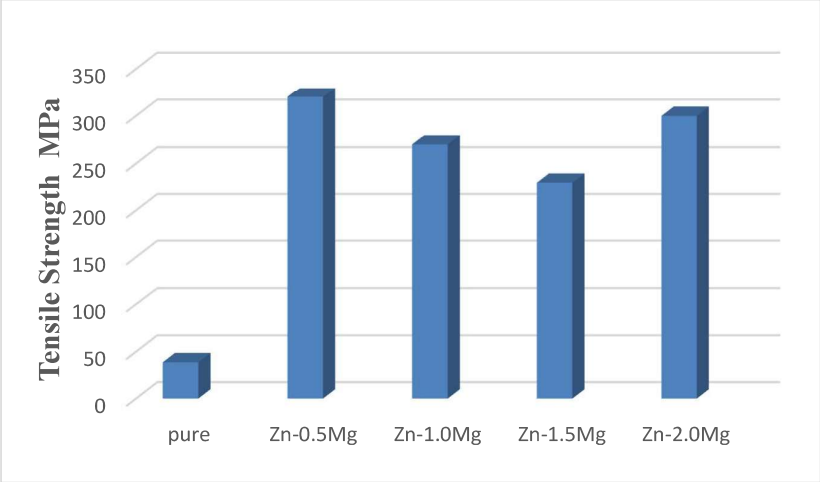

Fig.8 Tensile strength of the Zn alloy.

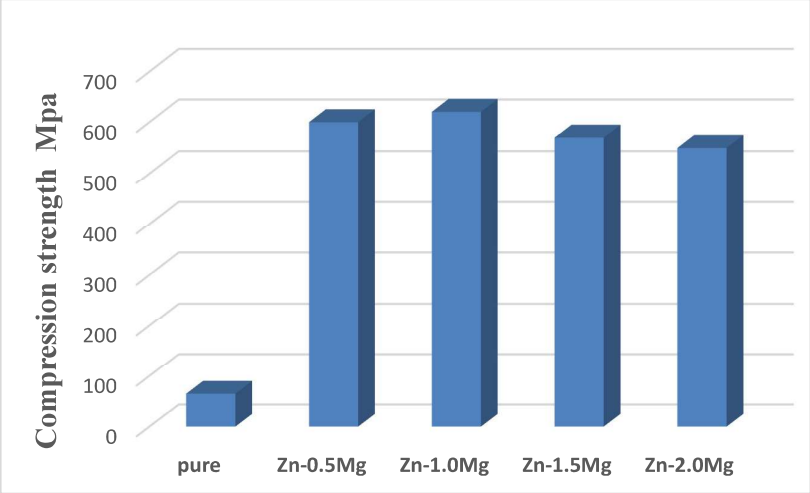

Fig.9 Compression strength of the Zn alloy.

Regarding to result, Hardness for zinc–0.5Mg in Fig.7 increased by 92% more than that of pure zinc. Increasing Mg ratio in alloy, increases hardness with percentage range from 2% to 10%.

Tensile strength and compression strength increased also with nearly ten times that of pure zinc. Tensile strength of zinc-XMg alloy was higher than strength of Titanium (UTS:220 Mpa) and pure magnesium (UTS: 160 Mpa) [40]. Compression strength for zinc–1.0Mg was more than zinc–0.5Mg by 3.33%. It concludes that zinc–0.5Mg alloy has improved mechanical properties and approached that needed to mimic bone and its mechanical values.

3.1.6. Electrochemical corrosion

Figure 10 shows the potentio-dynamic polarization curves of pure zinc, zinc–0.5Mg and zinc–1.0 Mg simulated body fluid (SBF) solution. The zinc–0.5Mg exhibit polarization behaviors better than pure zinc and zinc alloys with other Mg ratios. Corrosion parameters of pure zinc zinc–Mg alloys were mentioned in Table (4). The lowest corrosion rate is shown by zinc–0.5Mg then pure zinc, zinc–2.0Mg; zinc–1.5Mg and finally zinc–1.0 Mg. This is can be attributed to pores that aid

penetration of the SBF solution inside the plate sample causing increasing of corrosion rate. It was noticed that Mg and its good distribution works as an internal passive material lead to decrease of the corrosion rate.

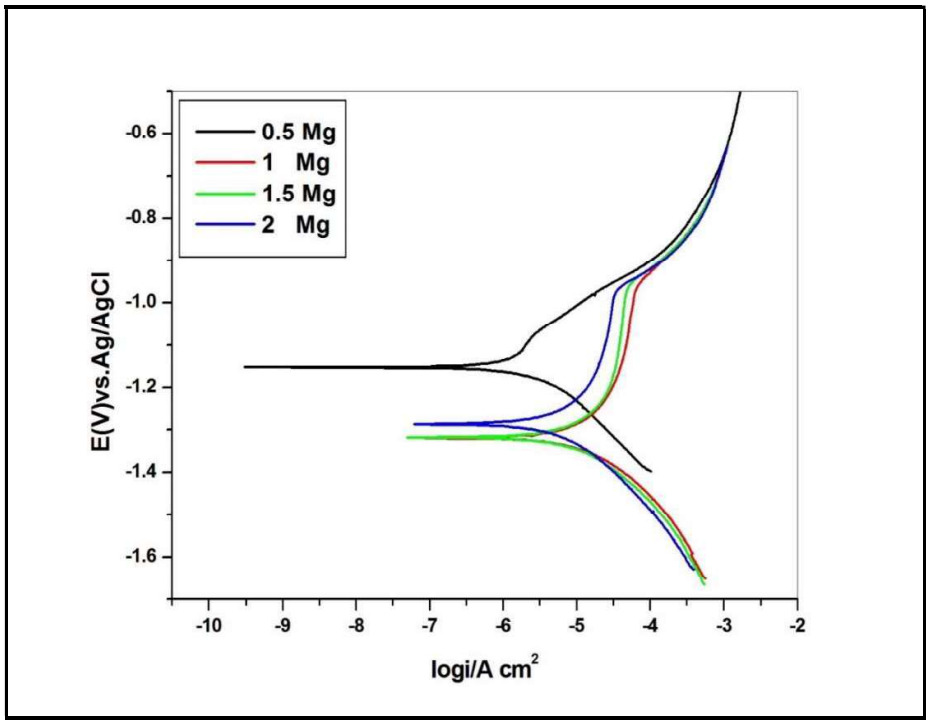

Fig.10 Potentio-dynamic polarization curves of Zn-XMg plates tested in SBF solution

Table4: Corrosion parameters of pure Zn and Zn alloy according to electrochemical measurements in SBF solution. The degradation rate was 0.0383 mm/year and 0.0525 mm/year for Zn-0.5 Mg alloy and pure zinc respectively. These degradation rates were lower than that for pure magnesium (0.54mm/year) [41-42].

Materials	$E_{corr, obs}$ (V)	I_{corr} ($\mu A/cm^2$)	Bc mV/dec	Ba mV/dec	Corrosion rate (mm/year)
Zn Pure	-1.0166	4.52197	112.507	59.9983	0.0525423
Zn-0.5 Mg	-1.0066	3.29511	194.013	59.1480	0.038287
Zn-1.0 Mg	-1.0505	10.9822	62.01529	179.714	0.127606
Zn-1.5 Mg	-1.1616	11.7417	134.026	82.0475	0.136431
Zn-2.0 Mg	-1.2874	30.1662	396.075	218.836	0.451722

Figure.11 shows Nyquist plots of the prepared plates in the SBF solution. Nyquist spectra showed semicircle behavior that related to a formation of complete passive barrier film on surface [43]. Semicircle in Nyquist spectra was seen as a characteristic for zinc [40]. The equivalent circuit was driven to simulate the EIS behavior in as shown in Figure.12, where R_1 and R_2 represent solution resistance and polarization resistance respectively. While, C_1 and C_2 represent the capacitance of the electrode surface, and polarization. These parameters were automatically derived by the software of the EIS testing instrument and listed in Table (5). It shows that

the highest resistance was for Zn-0.5Mg that indicate highest corrosion resistance for that alloy compared to pure zinc and other prepared alloys. It is noticed also that Zn-0.5Mg represents the lowest level of corrosion rate compared to the pure Zn or Zn-1.5Mg and Zn-2.0 Mg composite as shown in Figure.13. The Bode plots in Fig.14 shows that samples represents the same behavior with the best result for Zn-0.5Mg.

From immersion test, No obvious change in weight that support the conclusion of low degradation rate for Zn-XMg alloy.

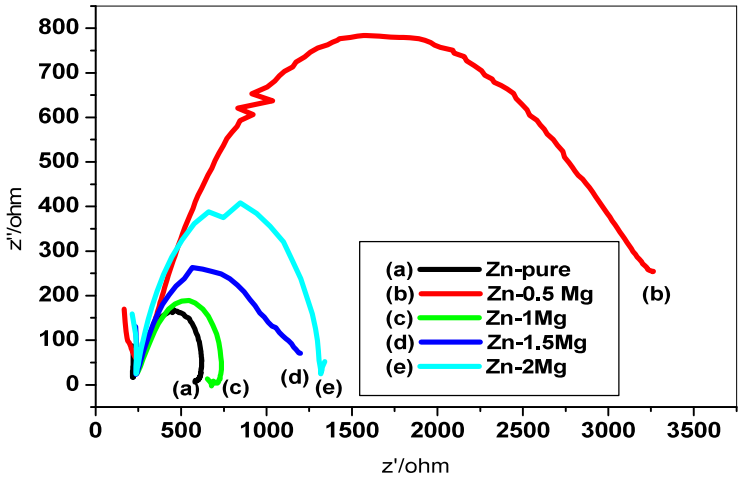

Fig.11: The Nyquist plotsof pure zinc and Zn-XMg composites in SBF.

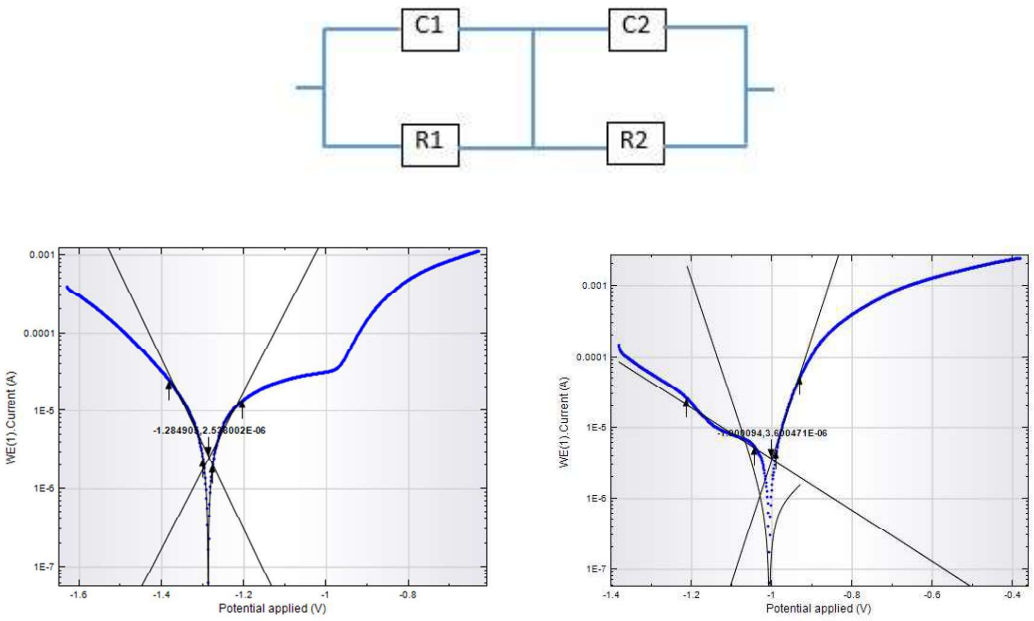

Fig.12: The equivalent circuit for curve-fitting of the EIS results and fitting curve

Table 5: Corrosion parameters of pure Zinc and Zinc-XMg alloys according to impedance measurements in simulated body fluid (SBF).

Materials	R1 (ohm)	R2 (ohm)	C1 (µF)	C2 (µF)
Zn Pure	374.63	231.39	6.09	2.60
Zn-0.5 Mg	276.15	688.64	2.37	3.54
Zn-1.0 Mg	261.05	442.73	2.39	3.14
Zn-1.5 Mg	261.45	529.74	2.98	4.98
Zn-2.0 Mg	257.75	599.42	3.59	2.79

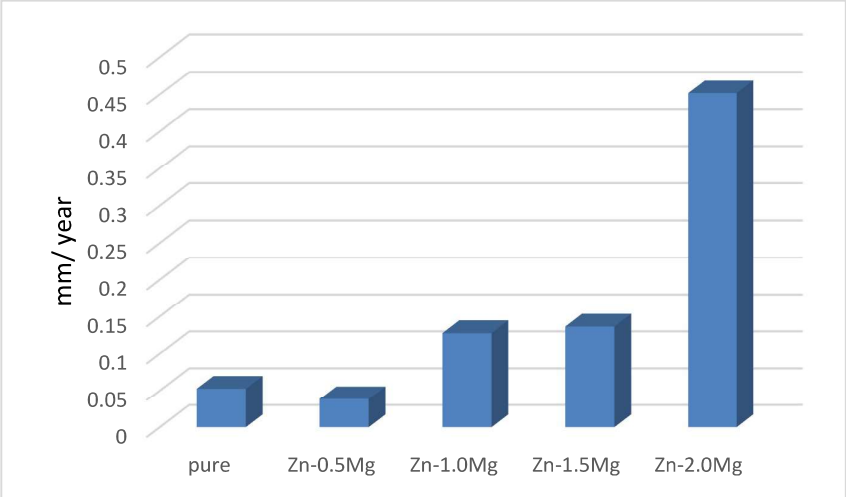

Fig.13: Corrosion rate of the Zn-XMg alloy.

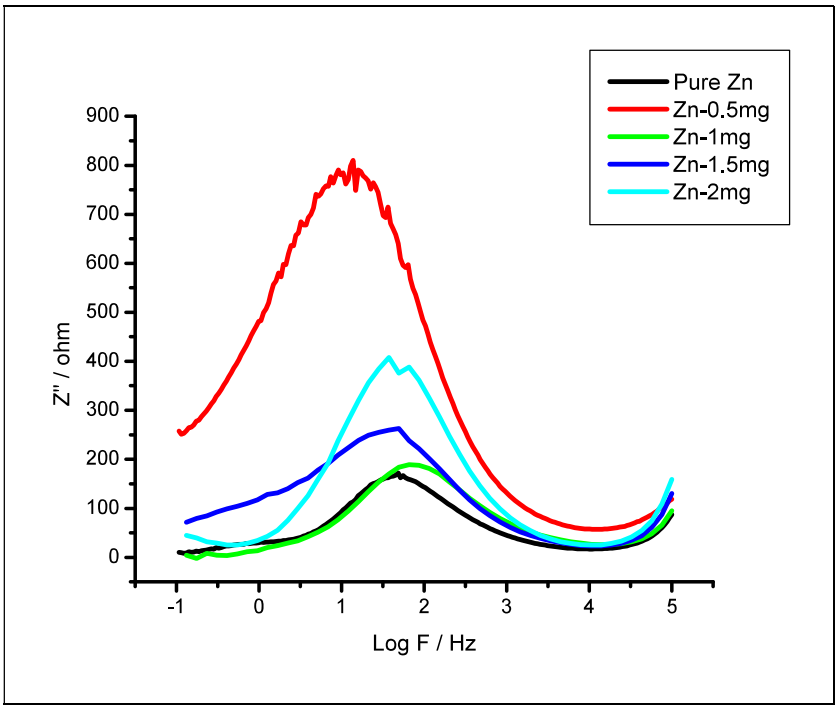

Fig.14 The Bode plots of pure Zinc and Zn-Mg alloys in SBF

4. Conclusions

Zinc-based alloys with different ratios of magnesium were fabricated for different medical applications with Mg percentages (0.5, 1.0, 1.5 and 2.0 wt. %). The study indicates high compatibility of zinc based-magnesium alloy for different medical applications. The mechanical properties and the degradation rate of Zinc alloy, are improved by adding Mg with different weight (0.5-2%). The properties were higher than that of the conventional used titanium plates or implants. Hardness, compression and tensile strength values enhanced corresponded to that of bone and manufactured plates. Zn-0.5Mg increases hardness from 39(±2.2) for pure zinc to 78 (±1.7). Tensile strength also increased up to 320MPa. Zinc based alloy was high compatibility comparing to other famous degradable plates. They have less degradable rate ranged from 0.05 to 0.45 mm /year while degradable rate for Mg alloys ranged from 0.5 till 1.5 mm /year [44]. Mg in zinc alloy works as an internal passive material that leads to decreasing of the corrosion rate. The mapping of Zn-Mg alloy also shows excellent distribution of Mg in alloys. The density decreased, mechanical properties and corrosion resistance improved with adding Mg. The most suitable alloy was Zn-0.5Mg as, it has the highest strength and high corrosion resistance that mean it has low degradable rate. In the future, more work is expected on Zinc based alloy as a bio-degradable bone plate to study the effect on growth of normal bone cells.

Acknowledgement

The authors wish to thank the researchers and the technicians of the Central Metallurgical R&D Institute (CMRDI).

References

[1] Michael Grau, et al. 2017 , In Vitro Evaluation of PCL and P(3HB) as Coating Materials for Selective Laser Melted Porous Titanium Implants, Materials2017, 10, 1344; doi:10.3390/ma10121344

[2] Q. Chen and G. A.Thouas, 2015 "Metallic implant biomaterials," Mater. Sci. Eng. R Reports, vol. 87, pp. 1–57.

[3] SANJAY SINGH, et al. 2015, Sol–Gel Derived Hydroxyapatite Coating on Mg-3Zn Alloy for

Orthopedic Application, 2015 The Minerals, Metals & Materials Society, JOM, Vol. 67, No. 4, 2015

[4] Dhyah Annur1 , Franciska P.L, et al. 2016, The synthesis and characterization of Mg-ZnCa alloy by powder metallurgy process Cite as: AIP Conference Proceedings 1725, 020032 (2016); https://doi.org/10.1063/1.4945486

[5] H.R.Bakhsheshi-RadaE.HamzahaM.DaroonparvaraM.A.M.YajidaM .Medrajb,2014, Fabrication and corrosion behavior of Si/HA nano-composite coatings on biodegradable Mg–Zn–Mn–Ca alloy. Surface and Coatings Technology, Vol. 258, pp.1090-1099

[6] L. F. Guleryuz, R. Ipek , I. Arıtman and S. Karaoglu, 2017,Microstructure and Mechanical Properties of Zn-Mg Alloys as Implant Materials Manufactured by Powder Metallurgy Method, AIP Conference Proceedings 1809, 020020 (2017)

[7] Wei Liu,‡a Jiaxing Wang et al., 2017, The improvement of corrosion resistance, biocompatibility and osteogenesis of the novel porous Mg–Nd–Zn alloy, J. Mater. Chem. B, 2017, 5, 7661—7674.

[8] R. NINKOVIC, M. BABIC, A. RAC, 2000, Zn-Al Alloys As Bearings Material, Tribology in industry, Volume 22, No. l&2 , UDK 69 1.77 l-0.34.5:621.82, 2000.

[9] C. N. Panagopoulos and A. G. Tsopani, 2011, Corrosion Behaviour of Zn-10Al-1.5Cu Alloy, International Journal of Corrosion, Vol. 2011, ID 540196

[10] Ying Liu , Bingheng Lu , and Zhixiong Cai, 2019, Recent Progress on Mg- and Zn-Based Alloys for Biodegradable Vascular Stent Applications, Journal of Nanomaterials, Vol.2019, ID 1310792.

[11] E. Mostaed, M. Sikora-Jasinska, J. W. Drelich, and M. Vedani, 2018, "Zinc-based alloys for degradable vascular stent applications," Acta Biomaterialia, vol. 71, pp. 1–23, 2018.

[12] H. Jin, S. Zhao, R. Guillory et al., "Novel high-strength, low-alloys Zn-Mg) and their arterial biodegradation," Materials Science & Engineering. C, Materials for Biological Applications, vol. 84, pp. 67–79, 2018.

[13] Z. Tang, J. Niu, H. Huang et al., "Potential biodegradable Zn-Cu binary alloys developed for cardiovascular implant applications," Journal of the Mechanical Behavior of Biomedical Materials, vol. 72, pp. 182–191, 2017.

[14] M. Noronha Oliveira et al., 2018 "Can degradation products released from dental implants affect peri-implant tissues?" J. Periodontal Res., vol. 53, no. 1, pp. 1–11.

[15] D. Liu, S. Hu, X. Yin, J. Liu, Z. Jia, and Q. Li, 2018, "Degradation mechanism of magnesium alloy stent under simulated human micro- stress environment," Materials Science & Engineering. C, Materials for Biological Applications, vol. 84, pp. 263–270, 2018.

[16] Jirí Kubásek, Drahomír Dvorský, 2019, The Fundamental Comparison of Zn–2Mg and Mg–4Y–3RE Alloys as a Perspective Biodegradable Materials, Materials 2019, 12, 3745.

[17] Li, H.F.; Xie, X.H.; et al., 2015, Development of biodegradable Zn-1X binary alloys with nutrient alloying elements Mg, Ca and Sr, Sci. Rep. 2015, 5, 10719.

[18] Kubasek, J.; Vojtech, D.; et al., 2016, Structure, mechanical characteristics and in vitro degradation, cytotoxicity, genotoxicity and mutagenicity of novel biodegradable Zn-Mg alloys. Mater. Sci. Eng. C Mater. 2016, 58, 24–35.

[19] Gong, H.; Wang, K.; Strich, R.; Zhou, J.G.,2015, In vitro biodegradation behavior, mechanical properties, and cytotoxicity of biodegradable Zn-Mg alloy. J. Biomed. Mater. Res. Part B Appl. Biomaterial, 2015, 103, 1632–1640.

[20] Murni, N.S.; Dambatta, M.S.; Yeap, S.K.; Froemming, G.R.A.; Hermawan, H., 2015, Cytotoxicity evaluation of biodegradable Zn-3Mg alloy toward normal human osteoblast cells. Mater. Sci. Eng. C Mater. 2015, 49, 560–566.

[21] Liu, X.W.; Sun, J.K.; Yang, Y.H.; Pu, Z.J.; Zheng, Y.F., 2015, In vitro investigation of ultra-pure Zn and its mini-tube as potential bioabsorbable stent material. Mater. Lett. 2015, 161, 53–56.

[22] Zberg, B.; Uggowitzer, P.J.; Loffler, J.F. ,2009, MgZnCa glasses without clinically observable hydrogen evolution for biodegradable implants. Nat. Mater. 2009, 8, 887–891.

[23] Bowen, P.K.; Guillory, et.al, Metallic zinc exhibits optimal biocompatibility for bioabsorbable endovascular stents. Mater. Sci. Eng. C 2015, 56, 467–472.

[24] Zhao, S.; Seitz, J, et.al, 2017, Zn-Li alloy after extrusion and drawing: Structural, mechanical characterization, and biodegradation in abdominal aorta of rat. Mater. Sci. Eng. C 2017, 76, 301–312.

[25] Bowen, P.K.; Seitz, J.M.; , et.al, 2018, Evaluation of wrought Zn-Al alloys (1, 3, and 5 wt % Al) through mechanical and in vivo testing for stent applications. J. Biomed. Mater. Res. Part. B Appl. Biomater. 2018, 106, 245–258.

[26] Kubasek, J.; Pospisilova, I.; Vojtech, D.; Jablonska, E.; Ruml, T. , 2014, Structural, mechanical and cytotoxicity characterization of as-cast biodegradable Zn-XMg (x = 0.8–8.3%) alloys. Mater. Tehnol. 2014, 48, 623–629.

[27] Katarivas Levy, G.; Goldman, J.; Aghion, E., 2017,The Prospects of Zinc as a Structural Material for Biodegradable Implants—A Review Paper. Metals 2017, 7, 402.

[28] Mostaed, E.; Sikora-Jasinska, M.; Drelich, J.W.; Vedani, M., 2018, Zinc-based alloys for degradable vascular scent applications. Acta Biomater. 2018, 71, 1–23.

[29] Bowen, P.K.; Shearier,et al,.,2016, Biodegradable Metals for Cardiovascular Stents: From Clinical Concerns to Recent Zn-Alloys. Adv. Healthc. Mater. 2016, 5, 1121–1140.

[30] Venezuela, J.; Dargusch, M.S.,2019, The influence of alloying and fabrication techniques on the mechanical properties, biodegradability and biocompatibility of zinc: A comprehensive review. Acta Biomater. 2019, 87, 1–40

[31] Gu, X.; Zheng, Y.; Zhong, S.; Xi, T.; Wang, J.; Wang, W. Corrosion of, and cellular responses to Mg–Zn–Ca bulk metallic glasses. Biomaterials 2010, 31, 1093–1103.

[32] Pan, F.; Bai, S.-L.; Zhang, E.-L.; Yu, G.-N.; Xu, L.-P. Degradation pattern and element distribution of WE43 magnesium alloy implanted in rats. Jiepou Xuebao 2010, 41, 425–429.

[33] Krause, A.; von der Hoh, N.; Bormann, D.; Krause, et al,.,2010,, A. Degradation behaviour and mechanical properties of magnesium implants in rabbit tibiae. J. Mater. Sci. 2010, 45, 624–632.

[34] Fathy A, Wagih A, Abu-Oqail A. Effect of ZrO2 content on properties of Cu–ZrO2 nanocomposites synthesized by optimized high energy ball milling. Ceramics International,Volume 45, Part A,2019, P:2319-2329

[35] Hossam M. Yehiaa, Ahmed El-Tantawy a, I.M. Ghayadb, Amal S. Eldesokyc , Omayma El-kady , 2020, Effect of zirconia content and sintering temperature on the density, microstructure, corrosion, and biocompatibility of the Ti–12Mo matrix for dental applications , J. materials research and technology, 2020; 9(4):8820–8833].

[36] A. International, “ASTM G31-72: Standard Practice for Laboratory Immersion Corrosion Testing of Metals,” United State, 2004.

[37] H. R. Bakhsheshi-Rad, E. Hamzah, H. T. Low, M. H. Cho, M. Kasiri-Asgarani, S. Farahany, A. Mostafa, M. Medraj, Thermal characteristics, mechanical properties, in vitro degradation and cytotoxicity of novel biodegradable Zn–Al–Mgand Zn–Al–Mg–xBialloys, Acta Metall. Sin. 30(3) (2017) 201–211.

[38] Ying Liu , 1,2 Bingheng Lu , 1 and Zhixiong Cai , Recent Progress on Mg- and Zn-Based Alloys for Biodegradable Vascular Stent Applications, Journal of Nanomaterials Volume 2019, ID 1310792, https://dobi.org/10.1155/2019/1310792

[39] El-Kady, Omyma, and A. Fathy. 2014"Effect of SiC particle size on the physical and mechanical properties of extruded Al matrix nanocomposites." Materials & Design (1980-2015) 54 : 348-353.

[40] Zhiping Guo, et al; 2020, Compressive Mechanical Properties and Shock-Induced Reaction Behavior of a Ti–29Nb–13Ta–4.6Zr, Alloy Metals and Materials International, 2020, 26:1498–1505.

[41] M. Bobby et al., 2017, Biocompatibility and biodegradation studies of a commercial zinc alloy for temporary mini-implant applications, SCientifiC ReportS | 7: 15605

[42] Yang, H.,Jia, B. et al. Alloying design of biodegradable zinc as promising bone implants for load-bearing applications, Nature Communications, volume 11, 401 (2020)

[43] Ruth S. MacDonald , Zinc and Health: Current Status and Future Directions , 2000, American Society for Nutritional Sciences.

[44] Ay a Mohamed, Ahmed M. El-Aziz , Hans-Georg Breitinger, Study of the degradation behavior and the biocompatibility of Mg–0.8Ca alloy for orthopedic implant applications , Journal of Magnesium and Alloys, 7 (2019) 249–257 b a Materials Engineering Department, German University in Cairo (GUC), 11835 New Cairo, Egypt